## 1. INTRODUCTION

It is important for most scientific analysis that how much radar energy reflects back from objects on the Earth. The procedure known as radiometric calibration is usually done by deciding calibration weights from corner reflectors and transponders. This report is for verifying the radiometric calibration of ASF (Alaska SAR Facility) processed RADARSAT product over the Antarctic Ice Sheet. This is primarily done by comparing the backscattered coefficient $\sigma^0$ of ASF product to similar data, collected from ERS-1 SAR and ERS-1 scatterometers obtained from the literatures. Once the verification is done, the procedure for determining the scale and offset to ingest amplitude (floating number) into RAMS (Radarsat Antarctic Mapping System) 16 bit DN (Digital Number) is discussed.

## 2. RADARSAT DERIVED BACKSCATTER DISTRIBUTION OVER ANTARCTICA

The geographic location of test sites is shown in Figure 1. Each rectangle represents approximate coverage of the RADARSAT data. The numbers in each rectangle represent ID which are listed in Table 1. The data are in slant range and each corresponding number of column and row represents numbers in slant range.

| ID | Orbit-frame | Beam mode | Incidence Angle (degree) | Image Size(column, row) |
|---|---|---|---|---|
| 1 | 9904-724 | ST2 | 24-31 | (6520,4096) |
| 2 | 10053-632 | ST2 | 24-31 | (6520,4096) |
| 3 | 9939-709 | ST2 | 24-31 | (6520,4096) |
| 4 | 10089-727 | ST2 | 24-31 | (6322,4096) |
| 5 | 9852-673 | ST3 | 30-37 | (5404,4096) |
| 6 | 10182-684 | ST4 | 34-40 | (5818,4096) |
| 7 | 9835-688 | ST5 | 36-42 | (6166,4096) |
| 8 | 9953-688 | ST6 | 41-46 | (6610,4096) |
| 9 | 9994-675 | EH4 | 54-57 | (6448,4096) |
| 10 | 10028-696 | ST2 | 24-31 | (6520,4096) |
| 11 | 9958-704 | ST2 | 24-31 | (6520,4096) |
| 12 | 9995-729 | ST2 | 24-31 | (6520,4096) |

Table 1. The summary of test RADARSAT data used in the report.

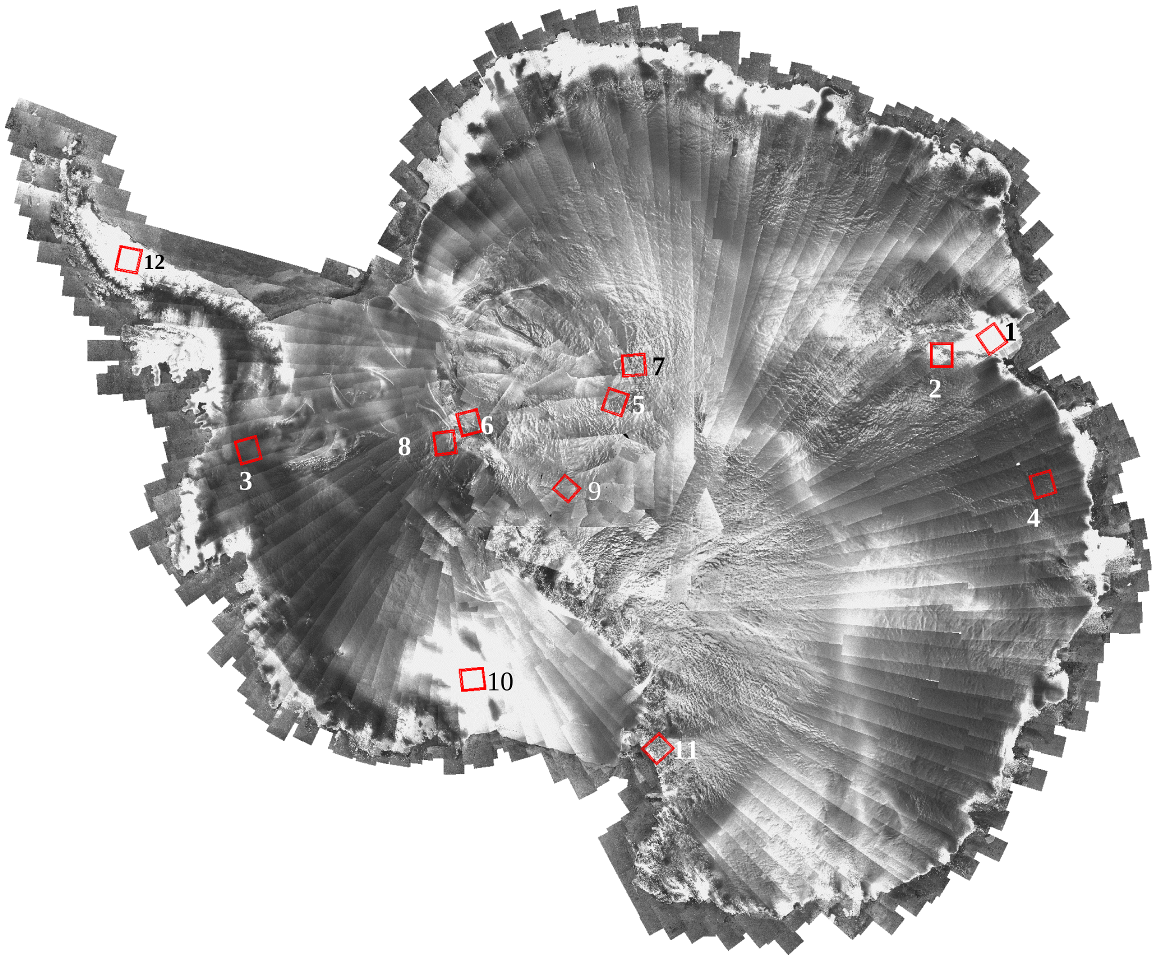


Figure 1. The geographic location map of 12 test RADARSAT sites.

## 2.1 Procedure

The data sets used are ASF processed RADARSAT and in a slant range. They consist of 16-bit (integer) pixel values. ASF provides an equation and per-image coefficients to convert these integer values to $\sigma^0$ (Kipple, 1998):

$$\sigma^0 \text{(in dB)} = 10 * \log(\mathit{power})$$
$$\text{power} = A_2*(DN*DN-A_1*N(r))-A_3 \qquad (1)$$

where, DN = 16-bit integer pixel value from ASF

A1 = calibration noise term

A2 = calibration linear term

A3 = offset (typically zero)

N(r) = noise as a function of range (interpolated from table)

Where:

| Beam | A1 | A2 | A3 |
|---|---|---|---|
| S2 | 2.174E+05 | 2.964E-7 | 0.0 |
| S3 | 2.0E+05 | 1.8E-7 | 0.0 |
| S4 | 3.0E+5 | 2.12E-7 | 0.0 |
| S5 | 2.0E+5 | 1.89E-7 | 0.0 |
| S6 | 3.0E+5 | 2.79E-7 | 0.0 |
| S7 | 2.6E+5 | 1.28E-7 | 0.0 |
| EH4 | 1.395E+5 | 1.438E-7 | 0.0 |

The typical noise vector as a function of range for each beam is shown in Figure 2. Each figure represents the average value of the CEOS noise vector for ST2, ST3, ST4, ST5, ST6, and EH4 beam, found in the radiometric data record. Each vector element represents 32 full resolution pixels and in-between we used linear interpolation method to estimate corresponding range noise vector.

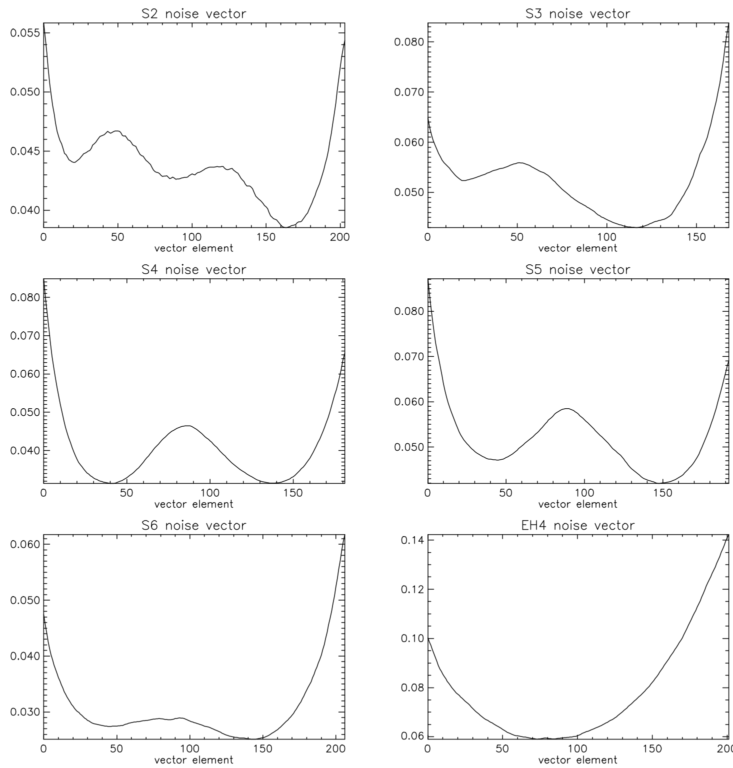


7

Figure 2. An estimate of noise vs. range for each beam.

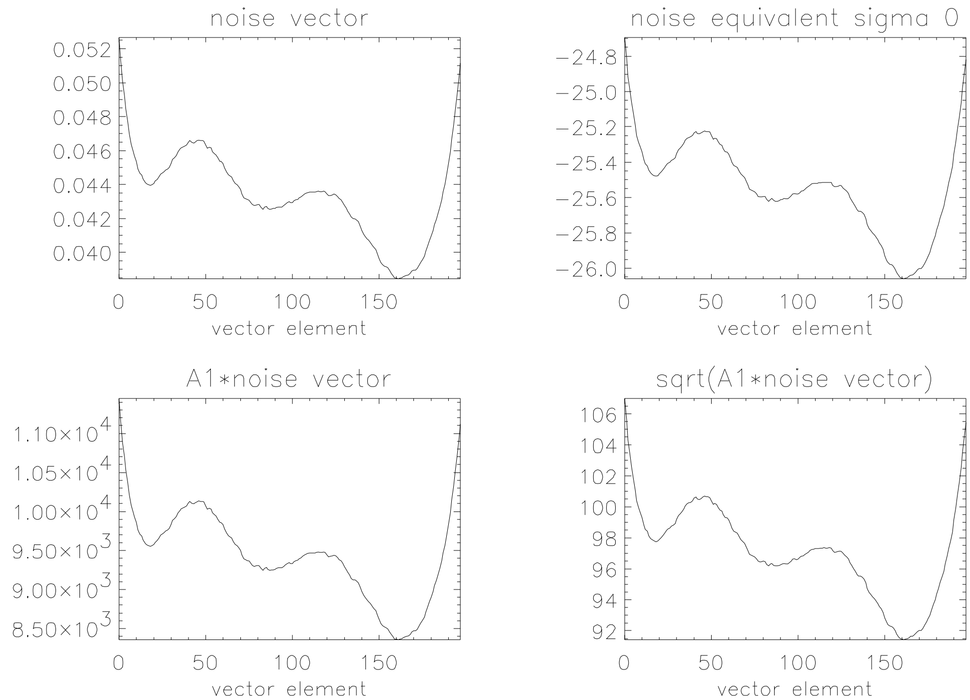


S2 beam

c

ST3 beam

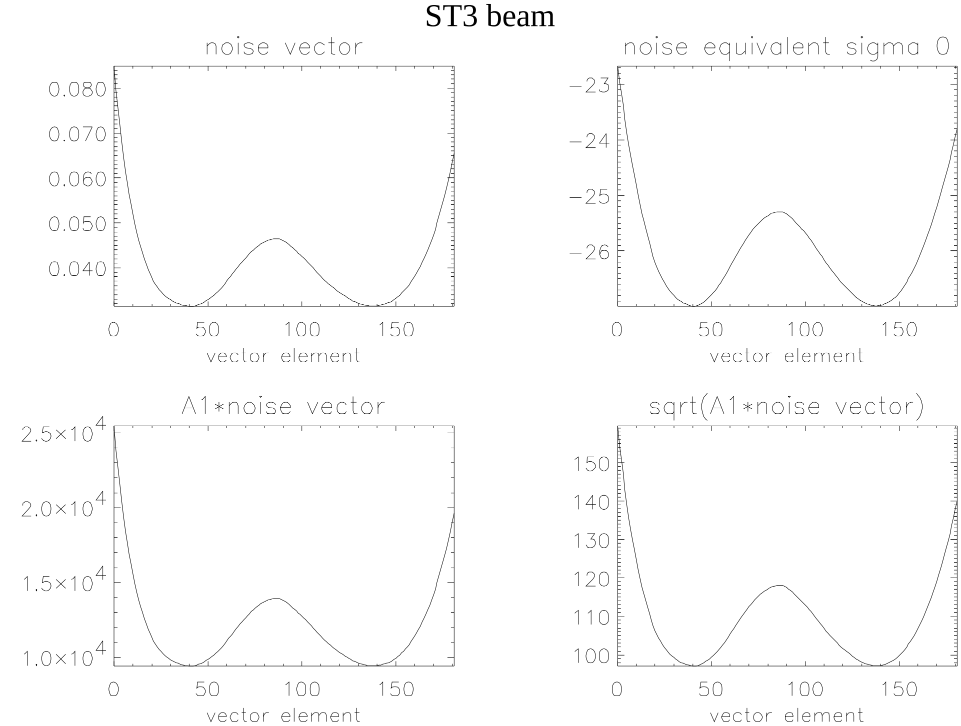


ST4 beam

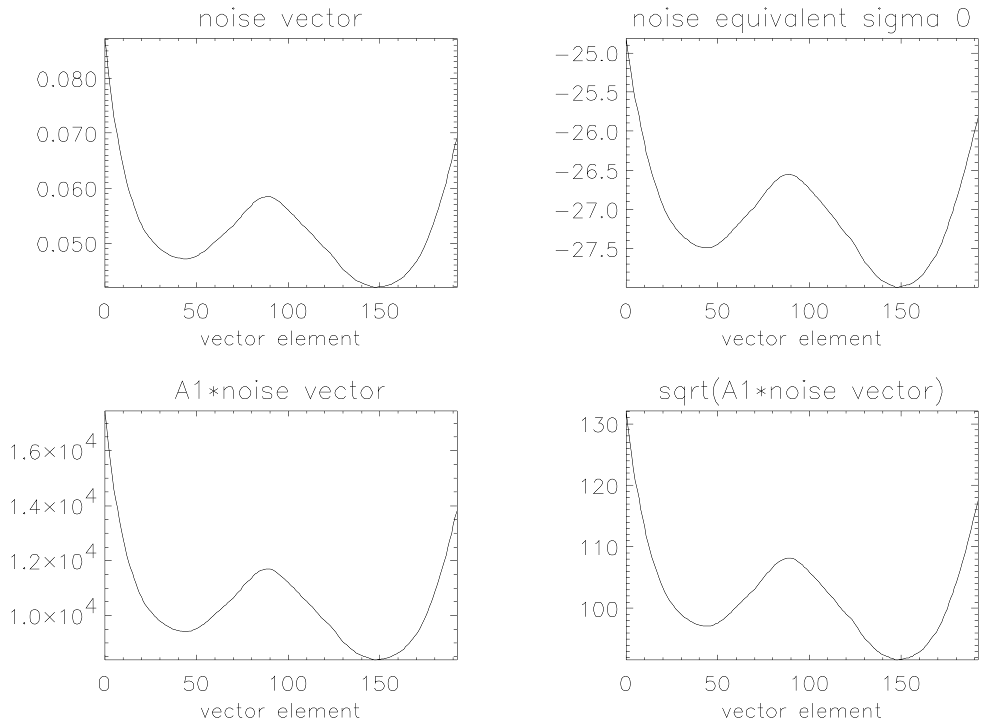


ST5 beam

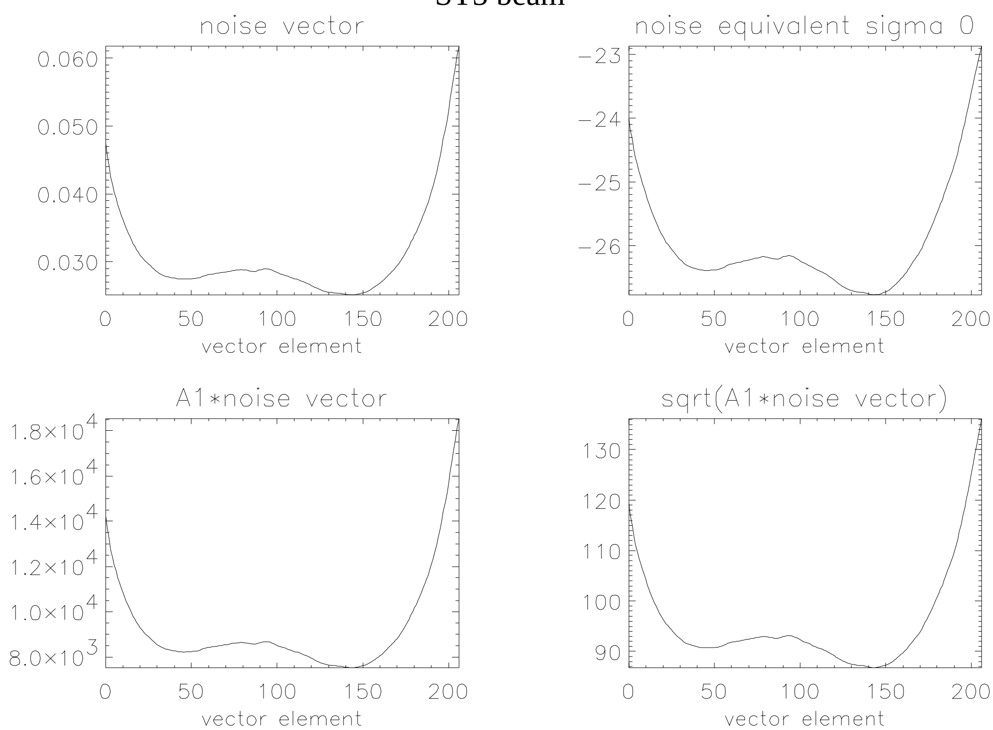


ST6 beam

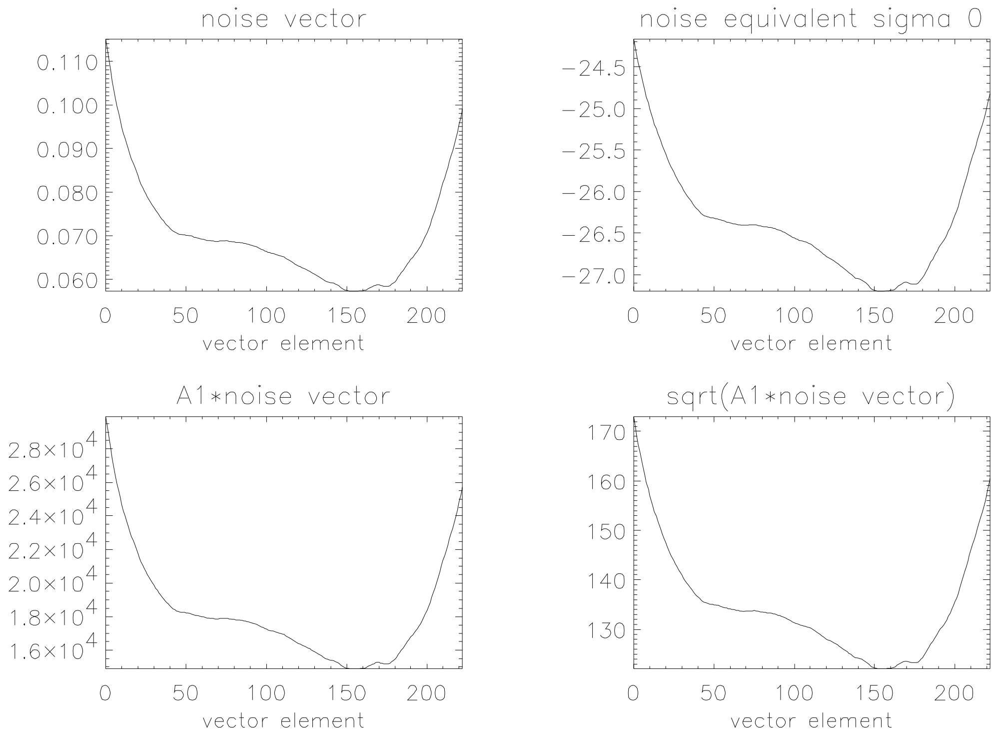


ST7 beam

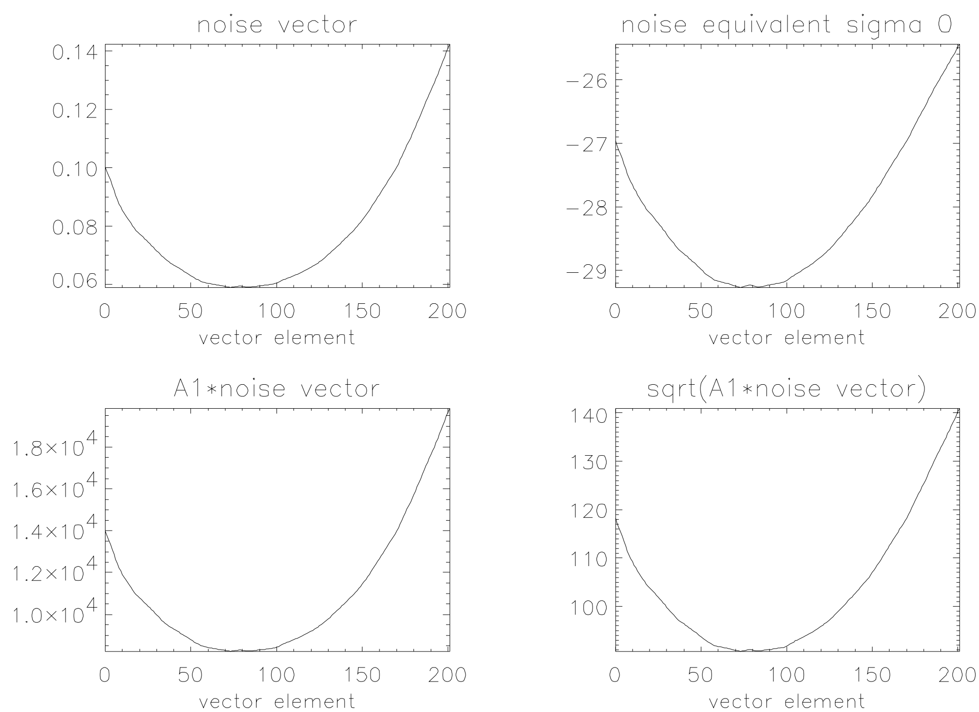


EH4 beam

### 2.2. Comparison of $\sigma^0$

Rott and Rack (1995) analyzed mean intensities, angular dependence, and azimuthal anisotrophy of backscattereing over Antarctica based on scatterometer of ERS-1, operating at 5.3 GHz and VV polarization for the period extending from April 5-30, 1993. The scatterometer covers about 50 km x 50 km ground area. In this report three sites are selected based on the location information listed in the literature. ID 1 and 2 in Figure 1 are two available closest data sets which correspond to two sites of percolation zone on Amery Ice Shelf in East Antarctica listed in the literature. ID 3 and 4 in Figure 1 are also two available closest data near the station Siple inWest Antarctica and an area in Princess Elizabeth Land.

Before compare the $\sigma^0$ value of the literature with ASF processes RADARSAT SAR, we must notice that RADARSAT SAR is C-band (5.3 GHz frequency or 5.6 cm wavelength) and HH polarization. Field measurements of C-band backscattering coefficients at different polarization over the Antarctic Ice Sheet shows that the difference between VV and HH polarization is at most a couple of dB difference at the incidence angle we are dealing with in this report (Rott and others, 1993). But there is no significant difference at the standard beam 2 (ST2) incidence angle range (24°–31°).

Figure 3 shows the slant range image of 9904-724 (ID-1). The DN (Digital Number) value distribution and RADARSAT-derived backscatter coefficient ($\sigma^0$) distribution binned at 0.1dB interval are also shown in Figure 3. The estimated value of $\sigma^0$ from Rott and Rack's plot using middle incidence angle of ST2 (~27°) is approximately 2dB. The estimated value of $\sigma^0$ from Figure 3 is about 0.5 dB. Similar approach was done on ID 2 (Figure 4), ID 3 (Figure 5), and ID 4 (Figure 6) area. The effect of azimuthal anisotrophy is also considered to estimate the $\sigma^0$ by calculating the illumination angle.

The result of comparison of $\sigma^0$ between the literature and our estimation is summarized in Table 2. The average difference between our estimation from RADARSAT and the literature is less than 1dB.

The relative standard deviation (standard deviation divided by mean) is used to estimate number of looks (Ulaby et al., 1982). For 4-looks case, the value of relative standard deviation is 0.28. We estimated the number of looks of the ASF processed RADARSAT by calculating the ratio of standard deviation and mean of original DN value. Two homogenous image data sets (ID 1 and ID 3) are used for the number of looks estimation. For 9904-724 (ID 1), the mean and standard deviation are 1883.2 and 503.5. The ratio becomes 0.26, which is close to 4 looks. For 9939-709 (ID 3), the mean and standard deviation are 298.9 and 86.7. Thus the ratio between standard deviation and mean becomes 0.29, which is close to 4 looks.

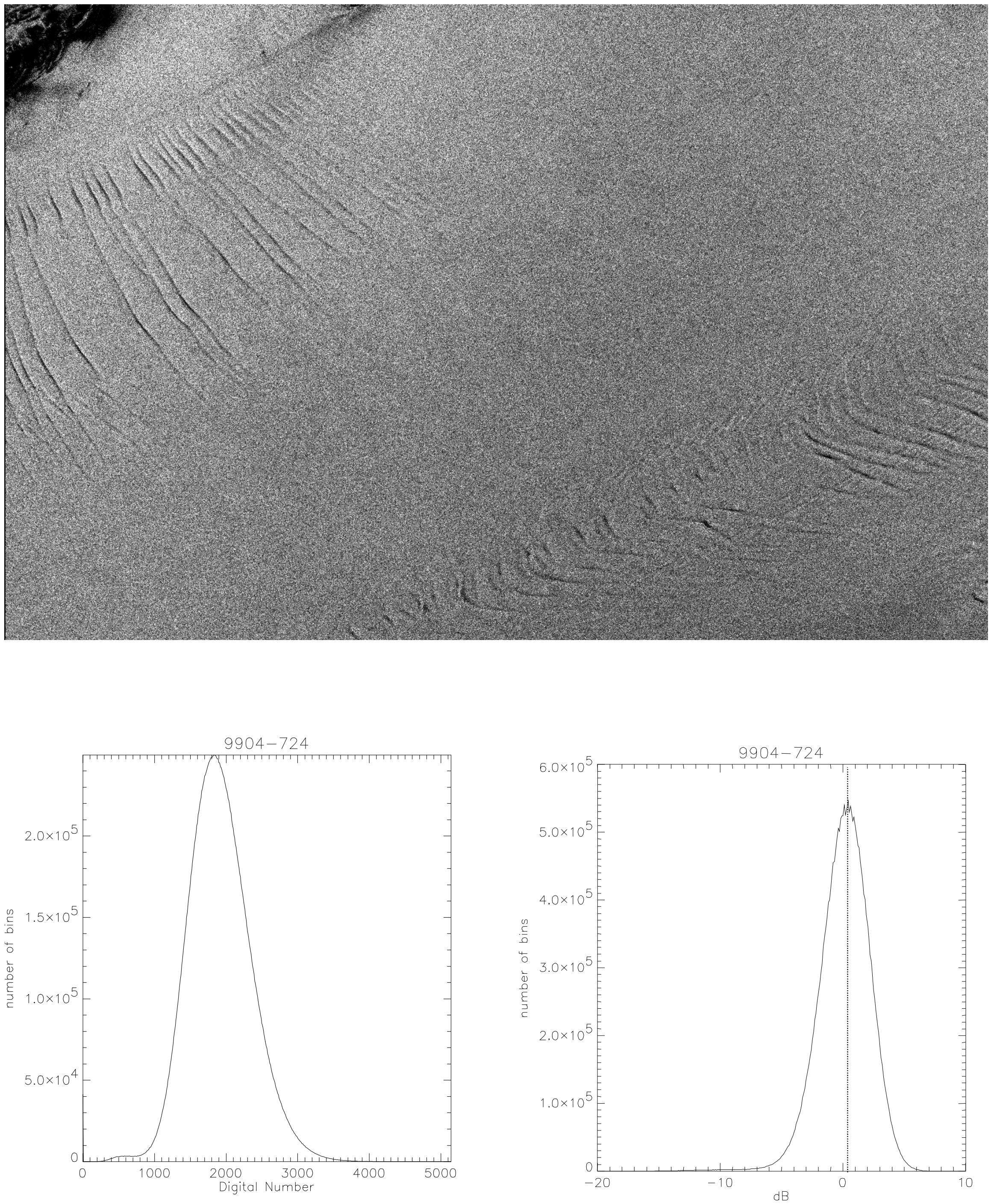


Figure 3. Slant range RADARSAT image over Amery Ice Shelf (ID 1), DN value distribution and $\sigma^0$ (in dB) value (corresponds to upper line in Fig.1 of Rott and Rack (1995))

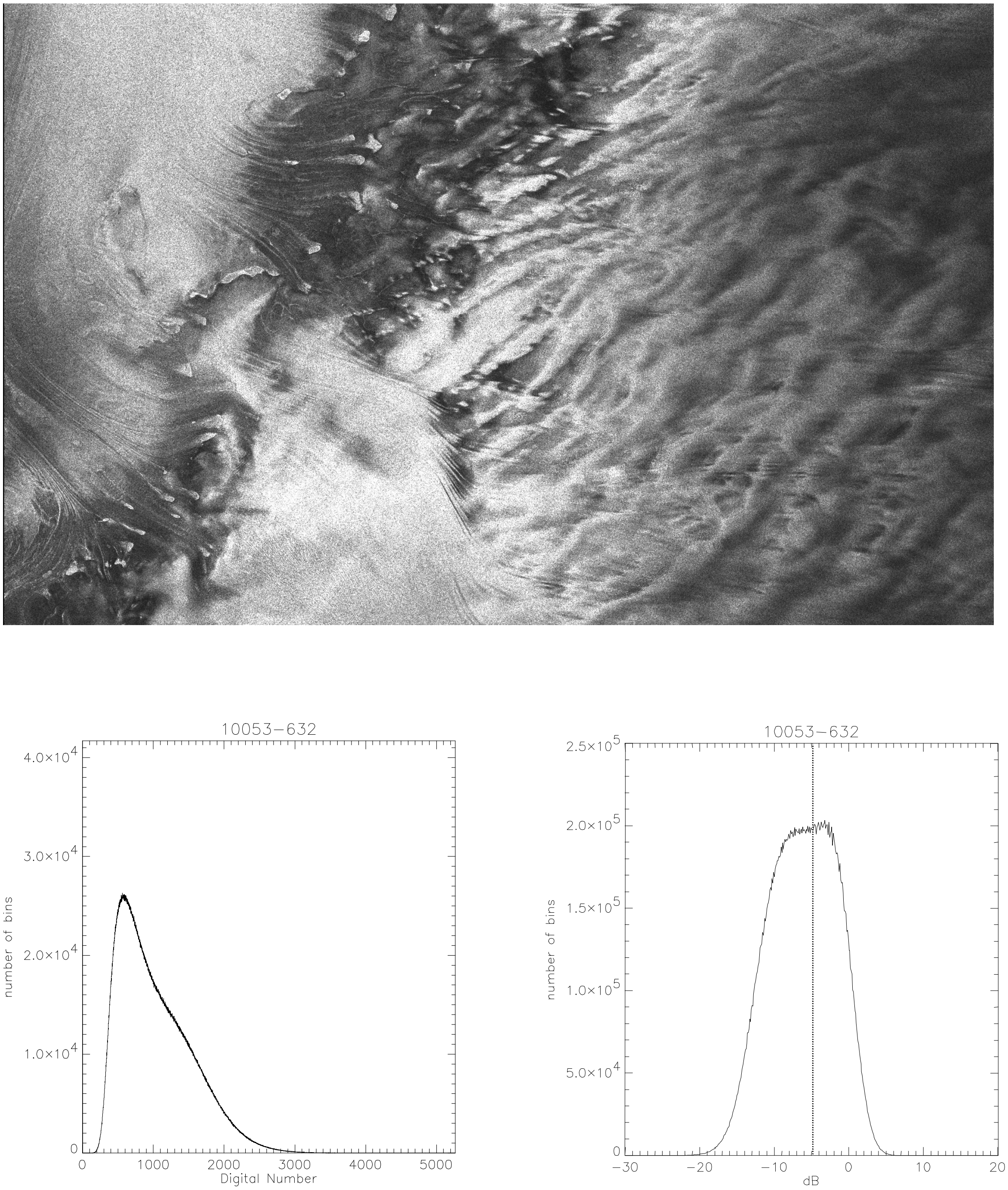


Figure 4. Slant range RADARSAT image over Amery Ice Shelf (ID 2), DN value distribution and $\sigma^0$ (in dB) value (corresponds to lower line in Fig.1 of Rott and Rack (1995))

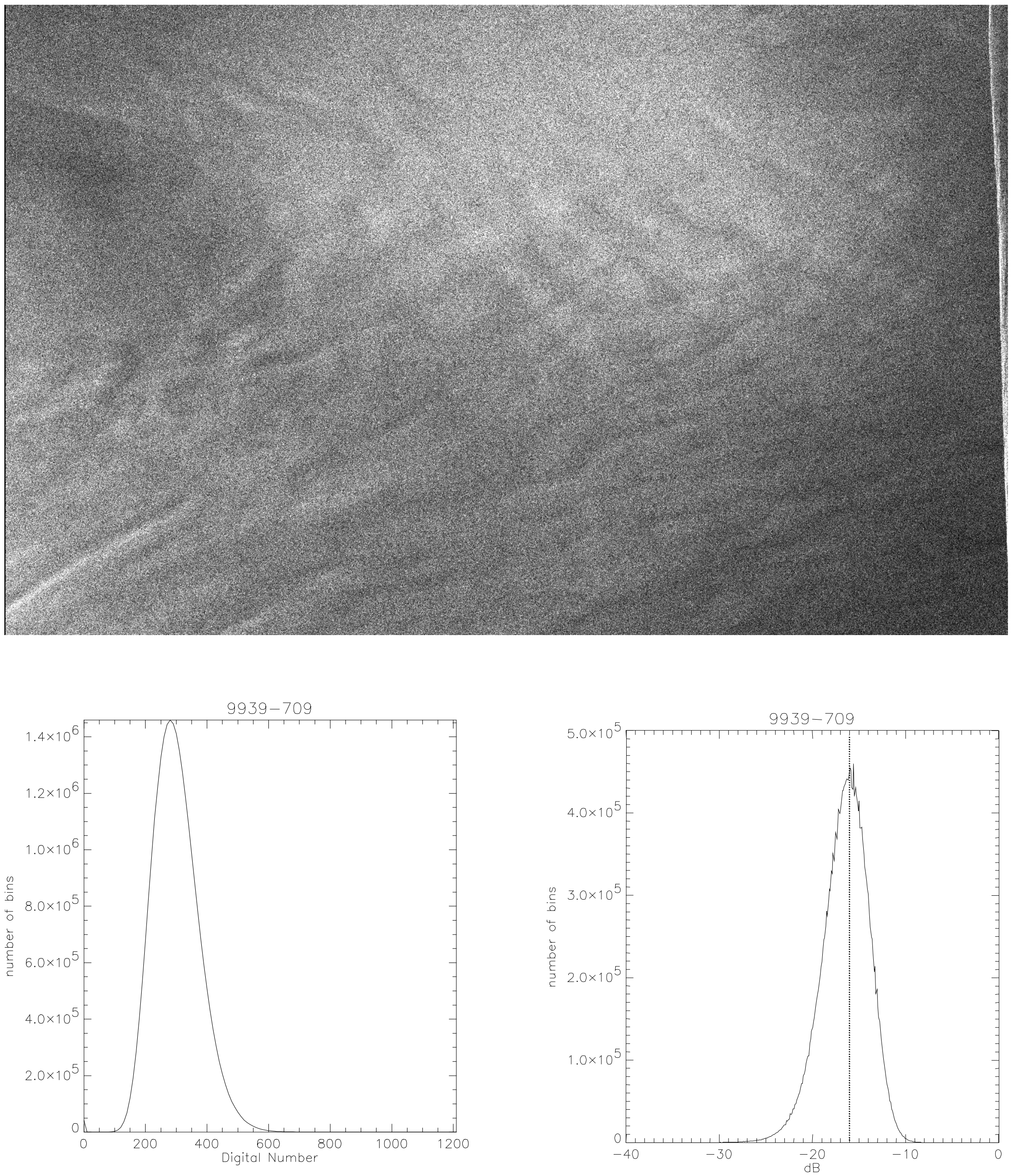


Figure 5. Slant range RADARSAT image for an area near Siple station (ID 3), DN value distribution and $\sigma^0$ (in dB) value (corresponds to Fig.2 of Rott and Rack (1995)). Track angle to the true north = 337.28°, thus satellite illumination angle = 337.28° -90° = 247.28° is used to estimate $\sigma^0$ from the plot.

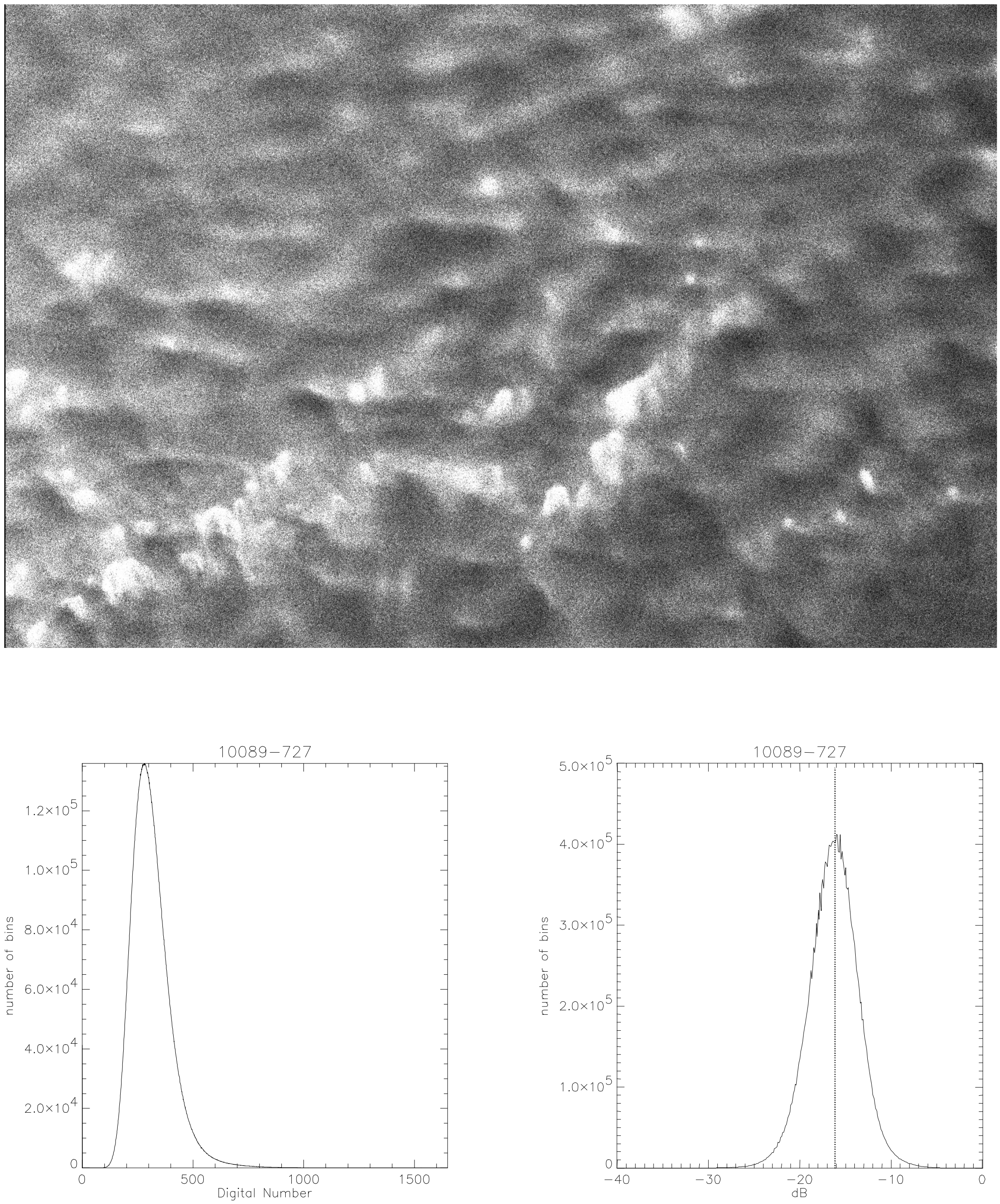


Figure 6. Slant range RADARSAT image for an area in Princess Elizabeth Land (ID 4), DN value distribution and $\sigma^0$ (in dB) value (corresponds to Fig.3 of Rott and Rack (1995)). Track angle to the true north = 327.54°, thus satellite illumination angle = 337.28° -90° = 237.54° is used to estimate $\sigma^0$ from the plot.

Table 2. Comparison of $\sigma^0$ between Rott and Rack (1995) and ASF processed RADARSAT data.

| ID | RADARSAT $\sigma^0$ (dB) | Radar Illumination Angle (degree) | Rott and Rack $\sigma^0$ (dB) |
|---|---|---|---|
| 1 | 0.5 | | 1.9 |
| 2 | -4.9 | | -4.2 |
| 3 | -16.0 | 247.28 | -15.5 |
| 4 | -16.1 | 237.54 | -15.4 |

## 2.3 Calculation of $\sigma^0$ using different beam modes

Using equation (1) and noise vector shown in Figure 2, we calculated $\sigma^0$ with different beam mode (ST2, ST3, ST4, ST5, ST6, EH4). The results of original DN value distribution and backscattered value from ID 5 to ID 12 is shown in Figure 7 through Figure 14.

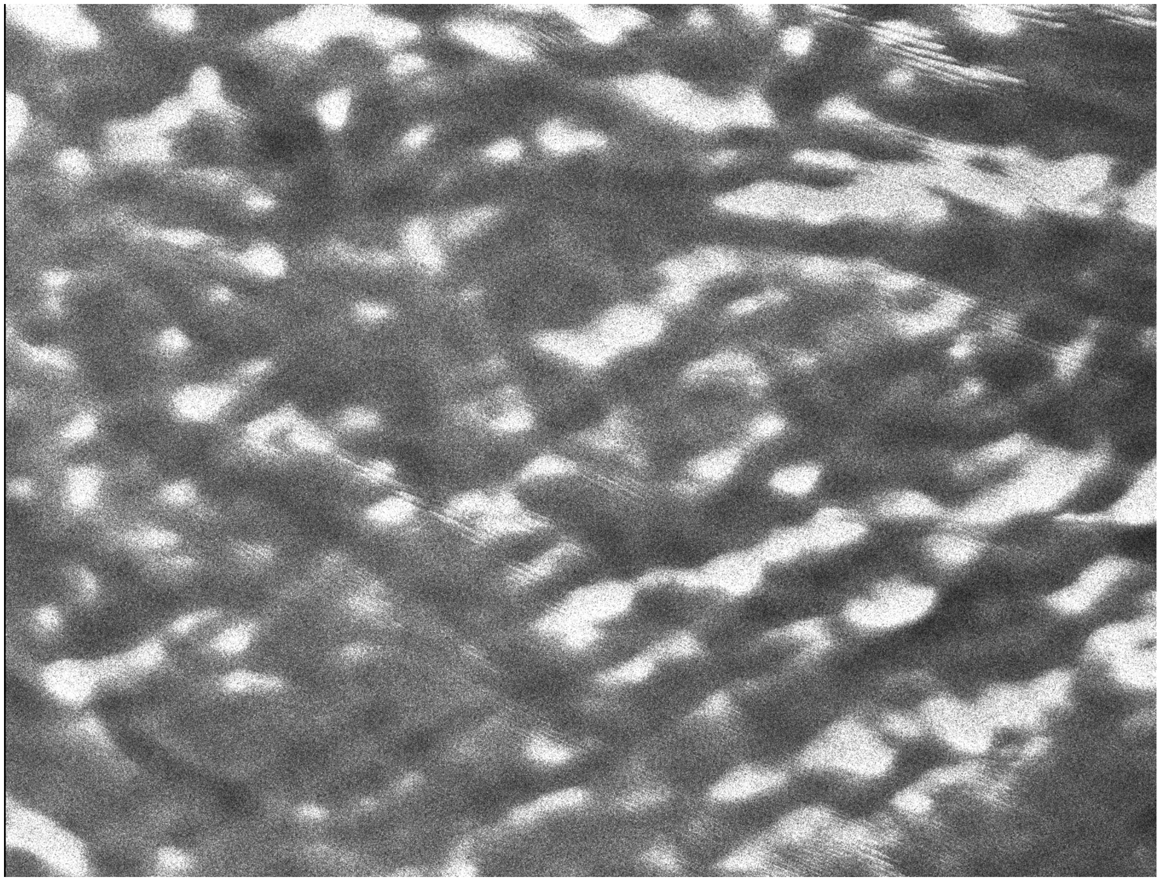

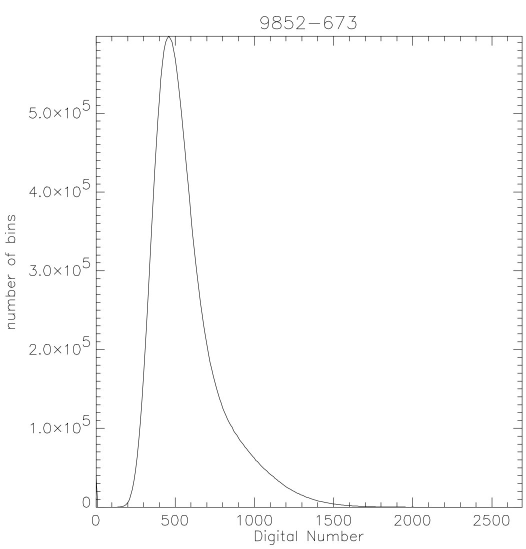


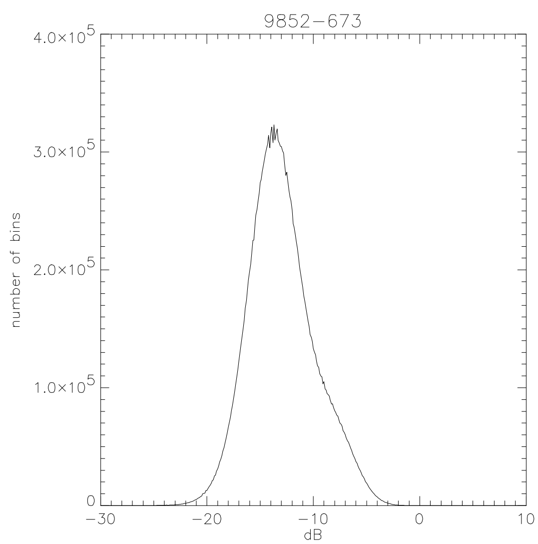


Figure 7. Slant range RADARSAT image for 9852-673 (ID 5, ST3), DN value distribution and $\sigma^0$ (in dB) value.

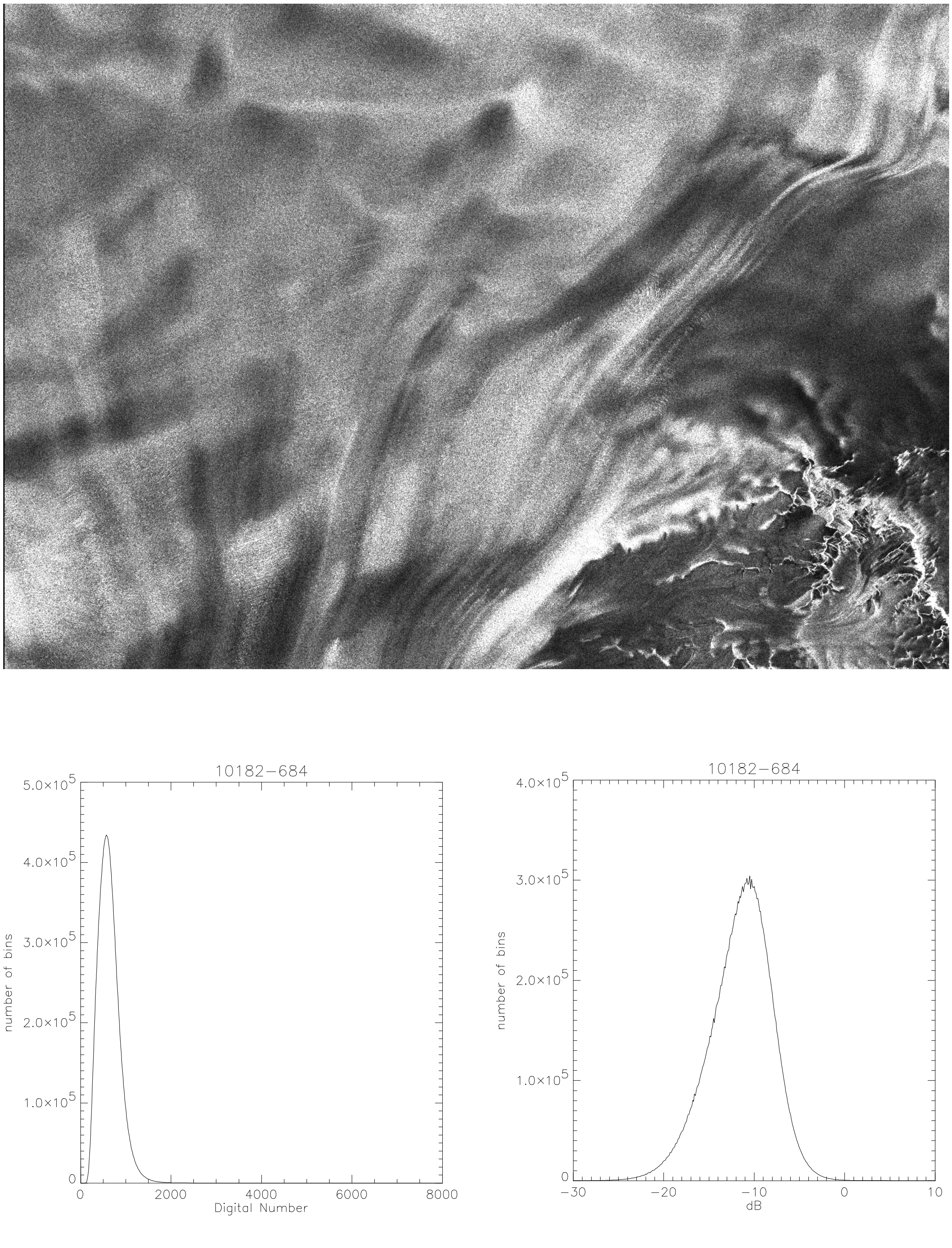


Figure 8. Slant range RADARSAT image for 10182-684 (ID 6, ST4), DN value distribution and $\sigma^0$ (in dB) value.

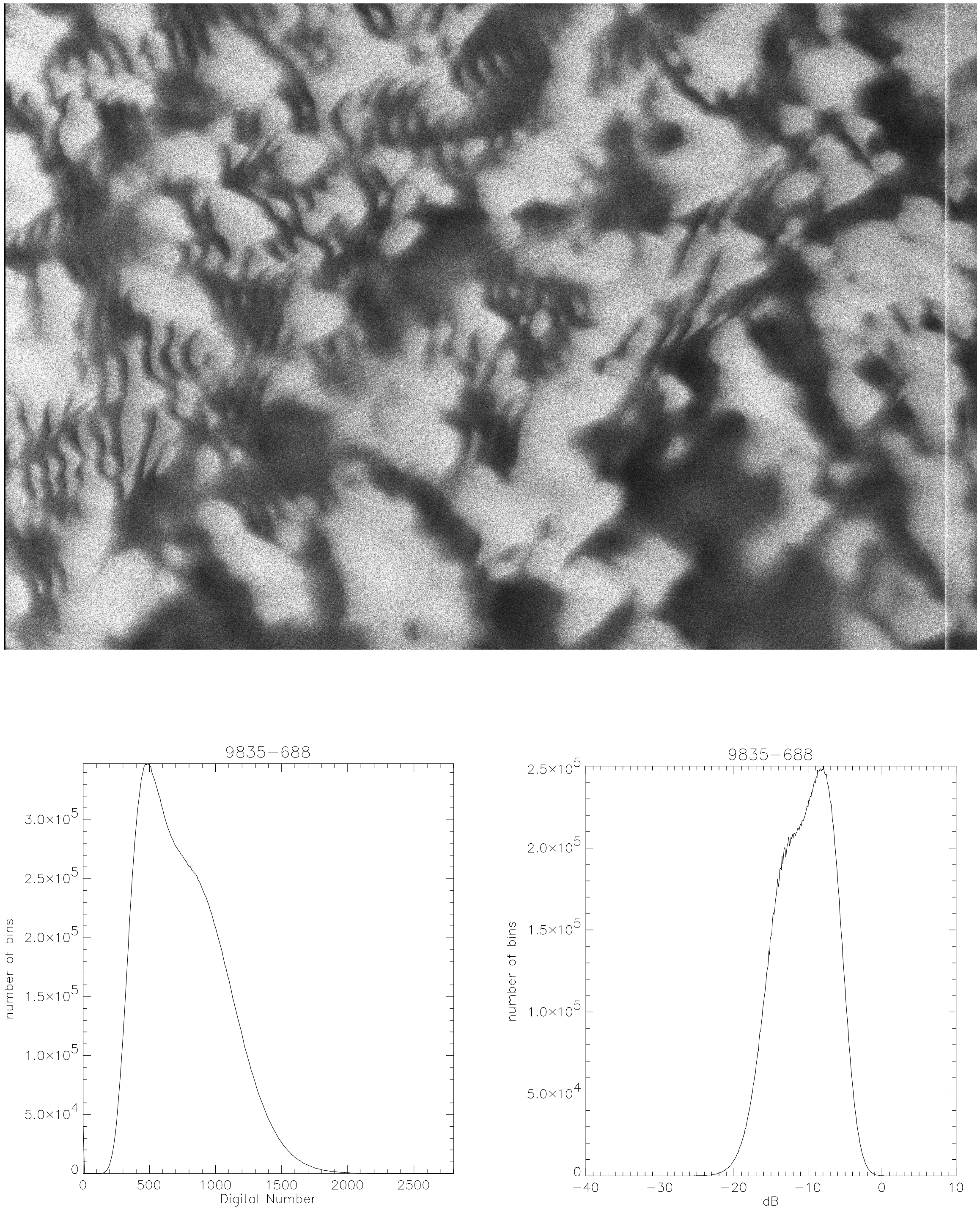


Figure 9. Slant range RADARSAT image for 9835-688 (ID 7, ST5), DN value distribution and $\sigma^0$ (in dB) value.

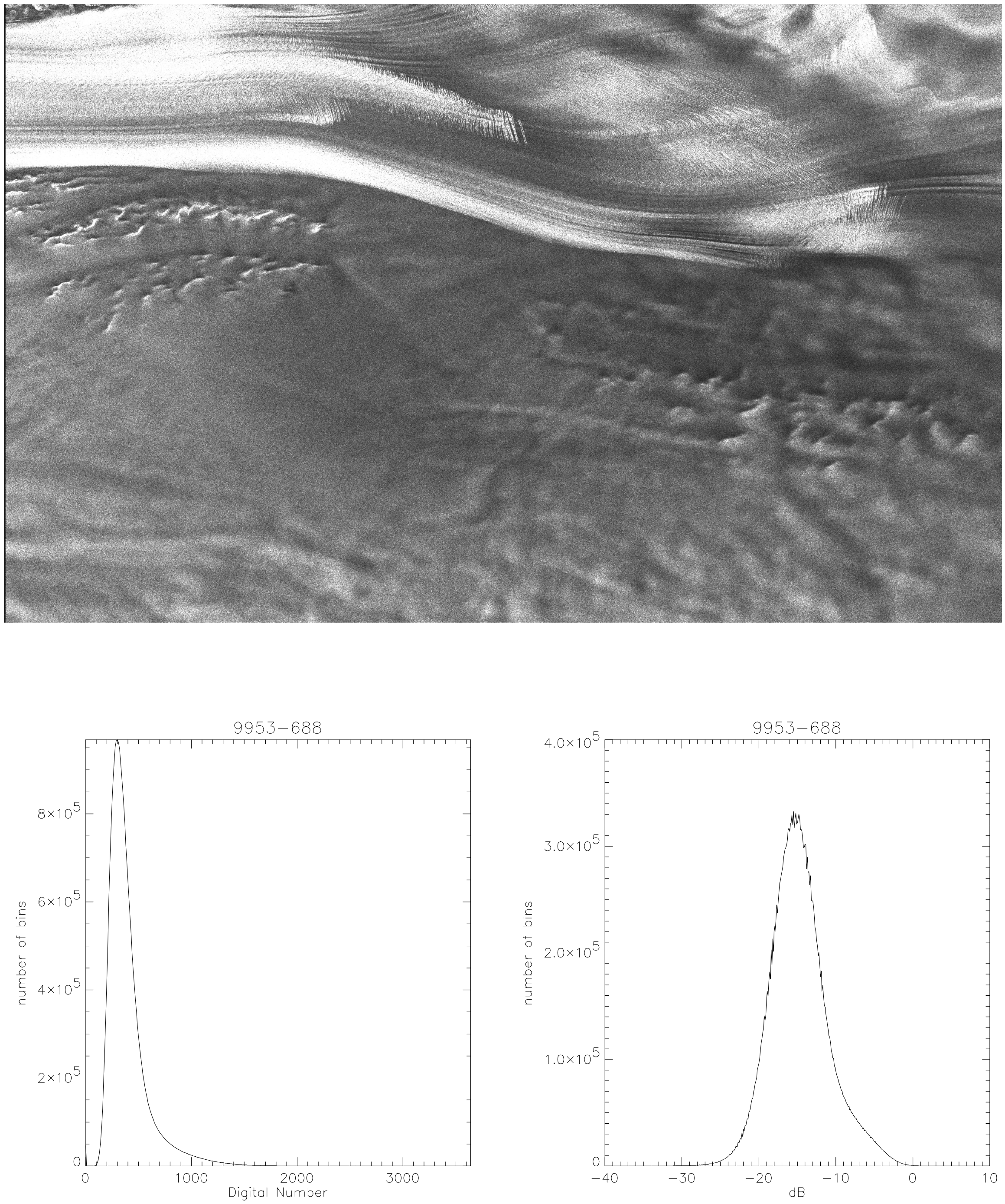


Figure 10. Slant range RADARSAT image for 9953-688 (ID 8, ST6), DN value distribution and $\sigma^0$ (in dB) value.

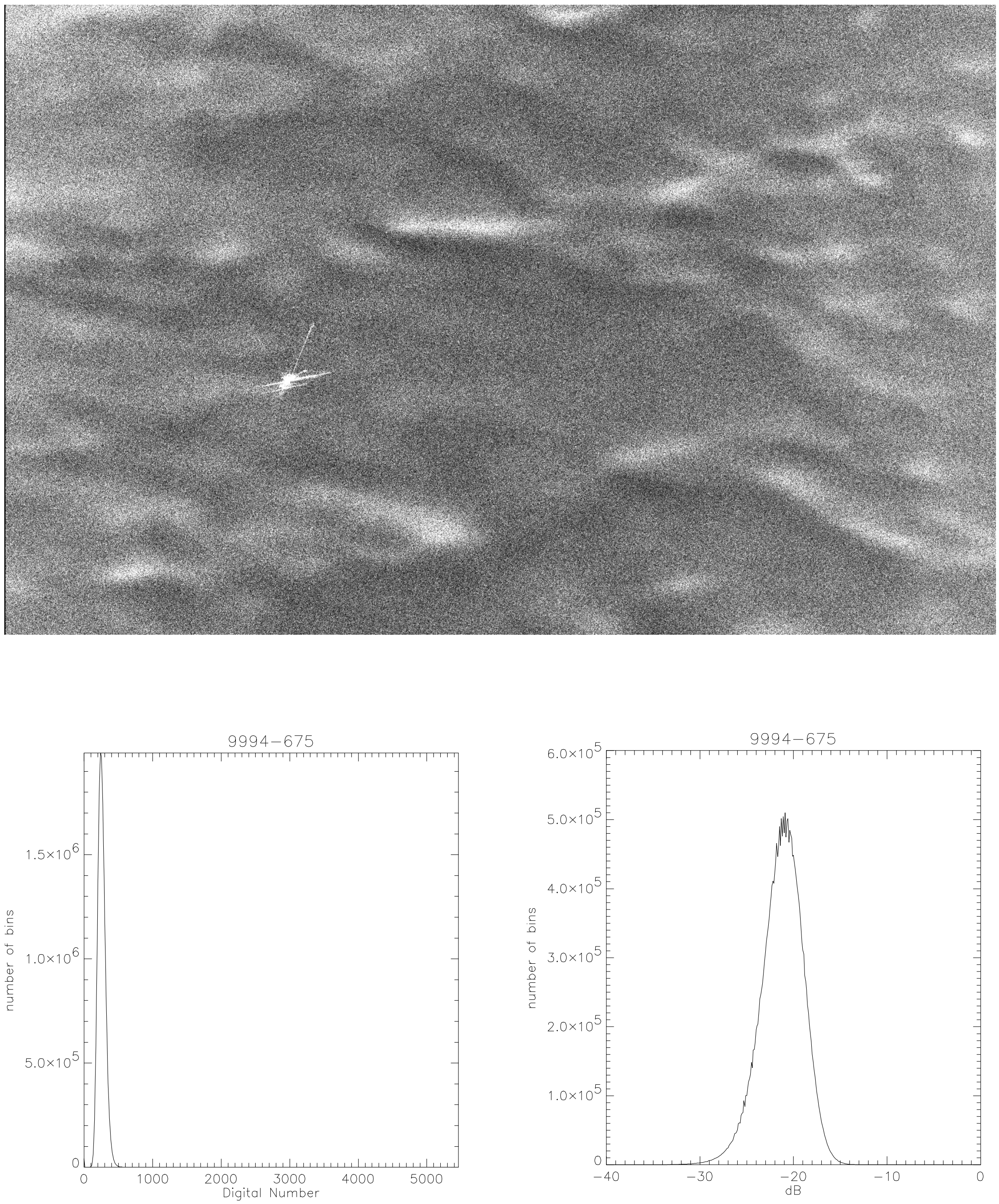


Figure 11. Slant range RADARSAT image for 9994-675 (ID 9, EH4), DN value distribution and $\sigma^0$ (in dB) value.

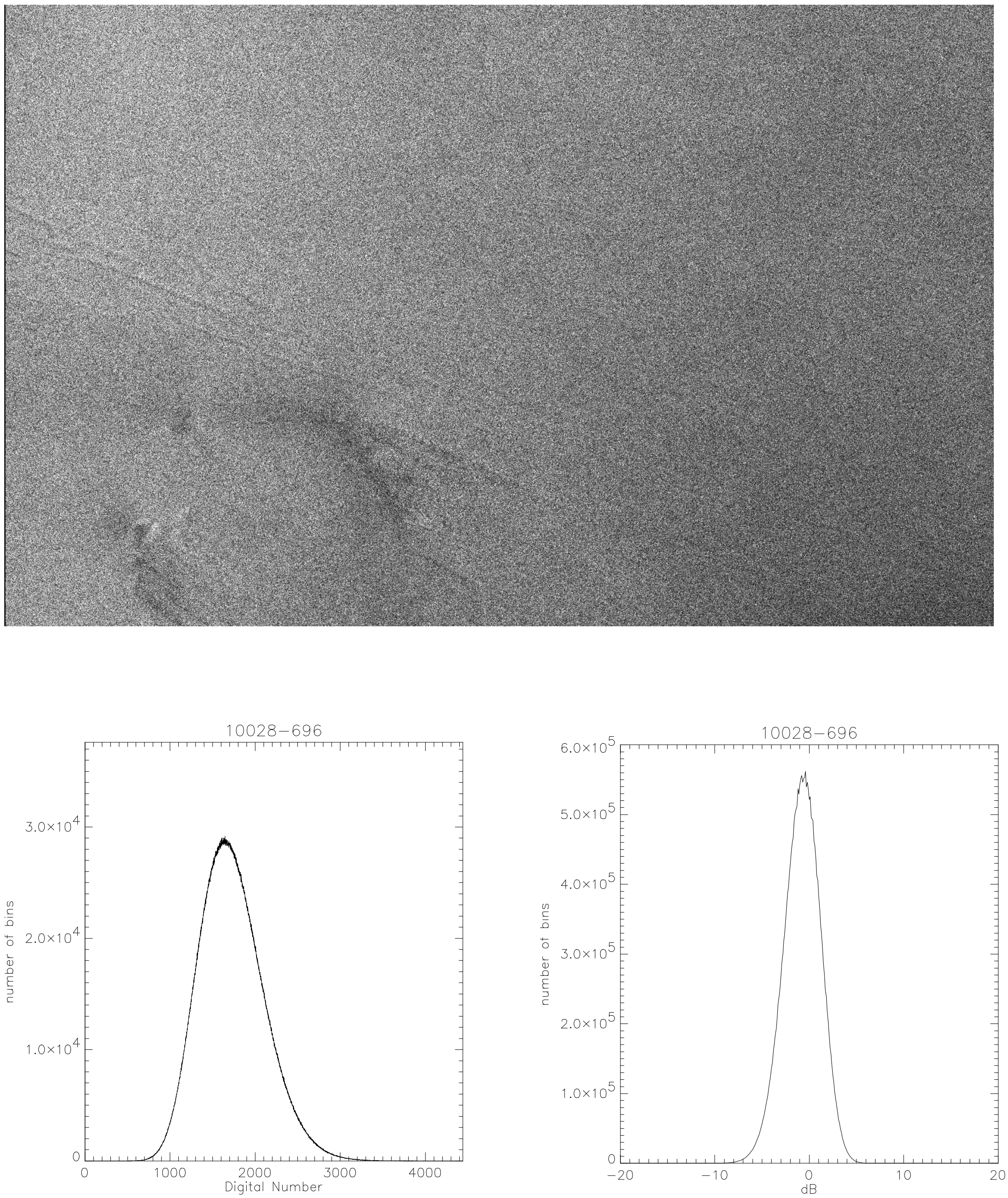


Figure 12. Slant range RADARSAT image for 10028-696 (ID 10, ST2), DN value distribution and $\sigma^0$ (in dB) value.

9958-704

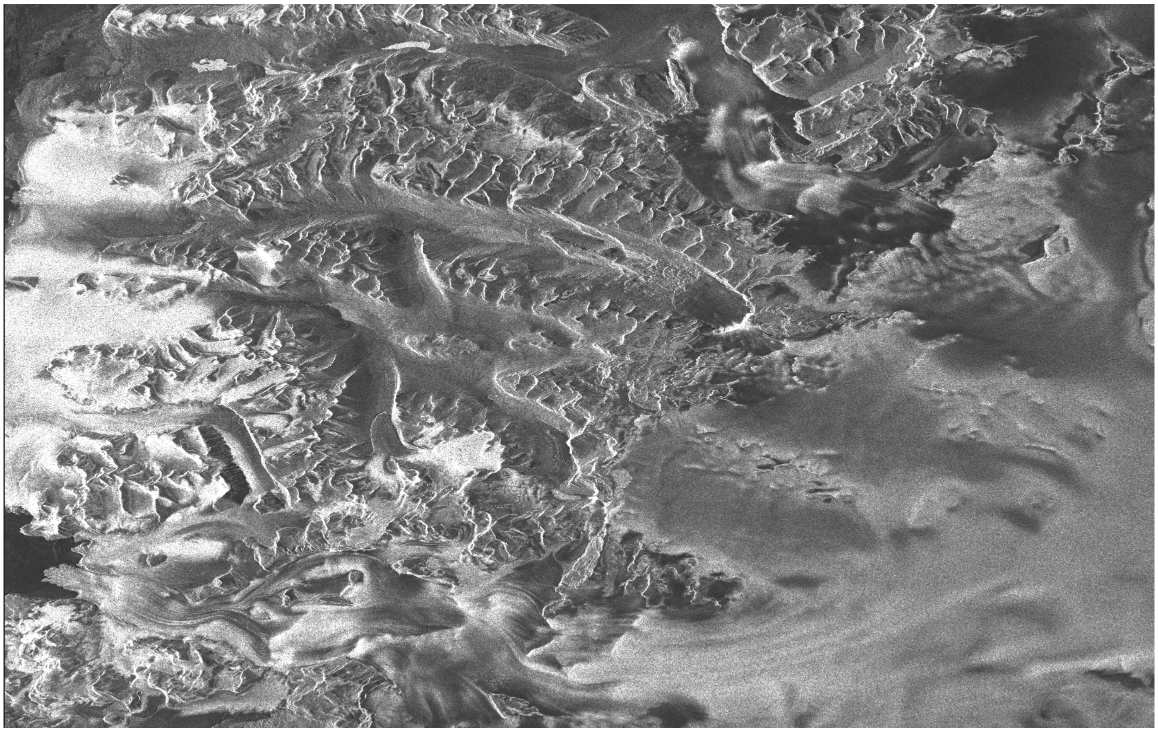

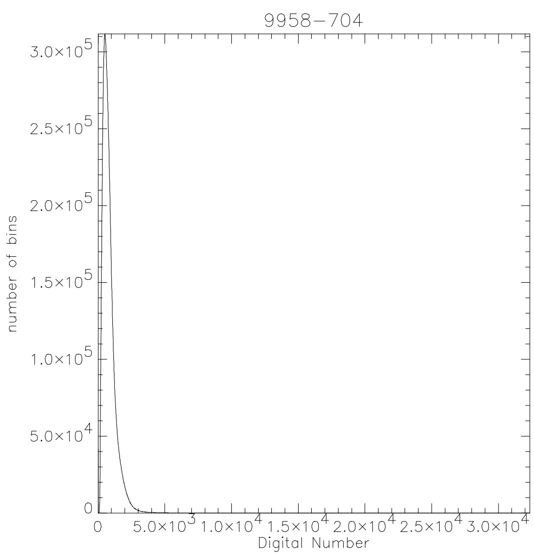


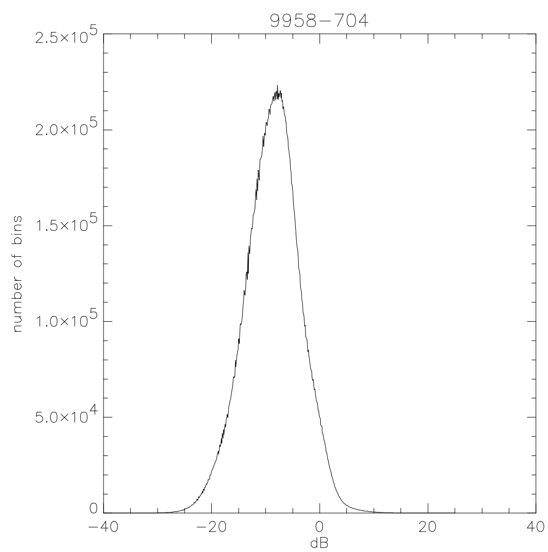


Figure 13. Slant range RADARSAT image for 9958-704 (ID 11, ST2), DN value distribution and $\sigma^0$ (in dB) value.

9995-729

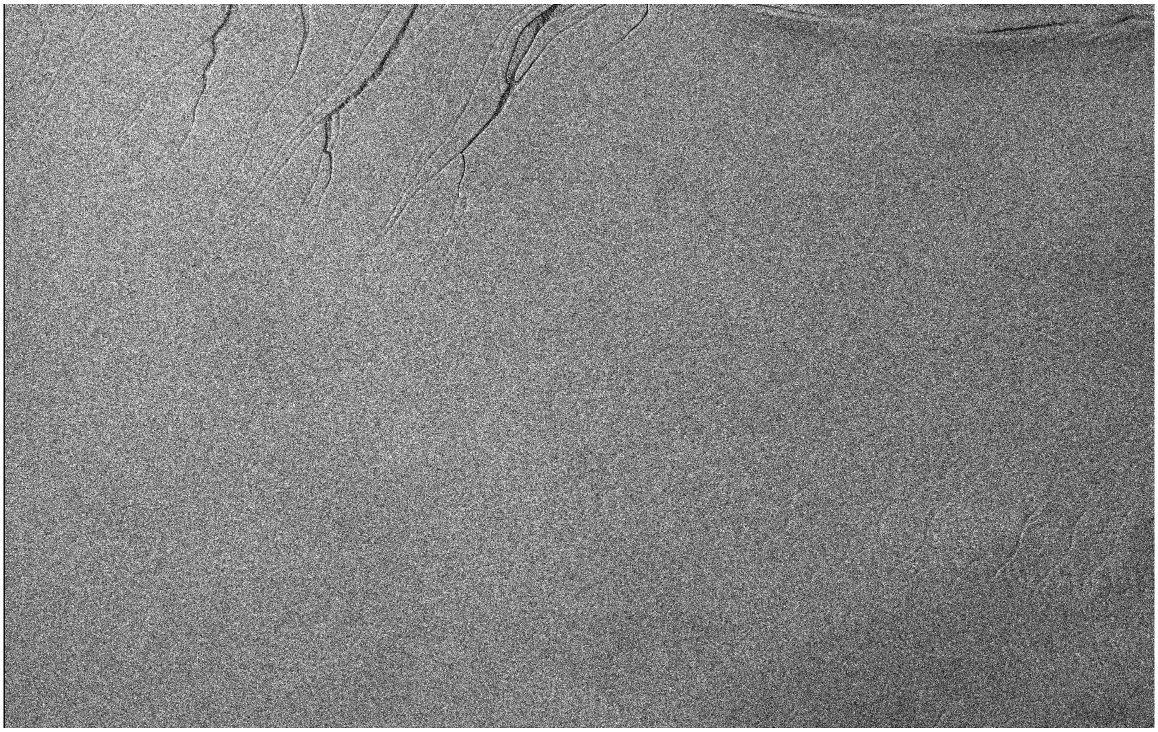

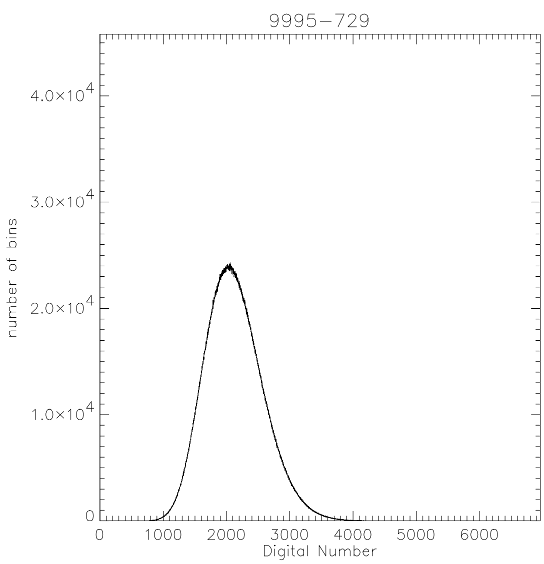


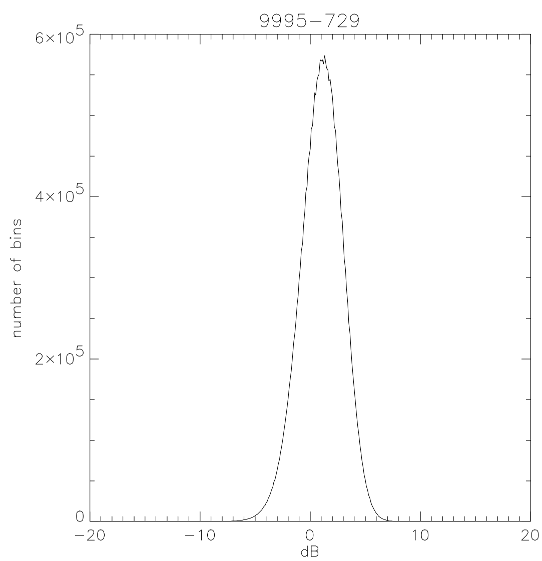


Figure 14. Slant range RADARSAT image for 9995-729 (ID 12, ST2), DN value distribution and $\sigma^0$ (in dB) value.

## 3. DETERMINATION OF AMPLITUDE SCALE AND OFFSET FOR RAMS

When ingesting ASF processed RADARSAT data, output for RAMS is 16 bit integer value. To do this RAMS uses amplitude scale and offset as following steps. First, calculate the power of each slant range pixel from equation (1). Then amplitude is calculated by square of root of power. The function called *rd_sar_load* in RAMS uses the following formula

$$\text{amplitude} = \sqrt{\text{power}} \tag{2}$$

$$\text{Dout} = (\text{signed short})[\text{amplitude\_scale} \cdot (\text{amplitude} + \text{amplitude\_offset}) + 0.5] \tag{3}$$

where, Dout : DN value used in RAMS. Amplitude offset is needed since the radiometric balancing may apply an offset to the data to get the proper balance and we do not want the data to go below zero.

It also automatically truncates the output values to the range of a non-negative 16-bit integer 0<= Dout <=32,767. The same scale and offset are used for all frames in a mission. To invert this value and recalaim power, we have

$$\begin{aligned} \text{amplitude} &= \frac{\text{Dout}}{\text{amplitude\_scale}} - \text{amplitude\_offset} \\ \text{power} &= \text{amplitude}^2 \end{aligned} \tag{4}$$

### 3.1 Procedure to decide amplitude scale and offset

Based on the above notation, we want to put our $\sigma^0$ range from -25 dB (noise floor) to as high as possible within the Dout range(~32,000)). Other suggested condition to determine the amplitude scale and offset is that minimum value of Dout is around 300. This minimum number restriction is for radiometric balancing. Another important factor to get the proper scale is to get the desired final histogram as close as possible to the original amplitude histogram. The final category to determine the scale is to make scale as big as possible within the range of Dout (~32,000), since the inverse of scale means the accuracy of amplitude we can recover from Dout DN value.

If power =0.003, then $\sigma^0$ = -25.22dB. This case amplitude becomes $\sqrt{0.003} = 0.05477$. In equation (3) to make inter arithmetic meaningful, the amplitude scale should be bigger than 100. Also we want to have our minimum RAMS ingested value (Dout) as a couple of hundred (~300).

After examining the amplitude histogram of original data and backscattering coefficient, we decide to choose, scale = 2000, and offset =0.1. The minimum Dout value is around $2000 \cdot (0.05477 + 0.1) = 309$. Using this amplitude scale and offset, the maximum amplitude we can get is $\frac{32,000}{2000} - 0.1 = 15.9$. This amplitude corresponds to power 252.81. This in turn corresponds to $\sigma^0 = 10 \cdot \log(252.81) = 24.0\,\text{dB}$. This maximum dB we can get is much higher value than that of our test sites.

### 3.2 Comparison of histogram of original DN and RAMS ingested DN

We compared the histogram of original ASF DN value with RAMS ingested DN value using amplitude scale 2000 and amplitude offset 0.1 we decide to use in RAMP. This is for verifying whether we can recover the original histogram distribution after RAMS ingestion using the scale and offset we determined in previous step. We tested for all beams used in RAMS including ST2, ST3, ST4, ST5, ST6, and EH4. Results are shown in from Figure 15 to Figure 22. We can see that the range of DN value before and after RAMS ingestion is quite similar. Also, the distribution of DN value before and after ingestion matches well. We conclude that the amplitude scale and offset we determined to use in RAMS is well fitted to the category mentioned earlier.

From equation (4) we can convert RAMS ingested DN value into $\sigma^0$. The procedure is as follows:

$$
\begin{aligned}
&\text{amplitude} = \frac{\text{RAMS ingested DN}}{\text{amplitude scale}} - \text{amplitude offset} \\
&\text{power} = \text{amplitude}^2 \\
&\sigma^0 = 10 \cdot \log(\mathit{power})
\end{aligned}
\tag{5}
$$

where, amplitude scale = 2000, amplitude offset = 0.1 for RAMS.

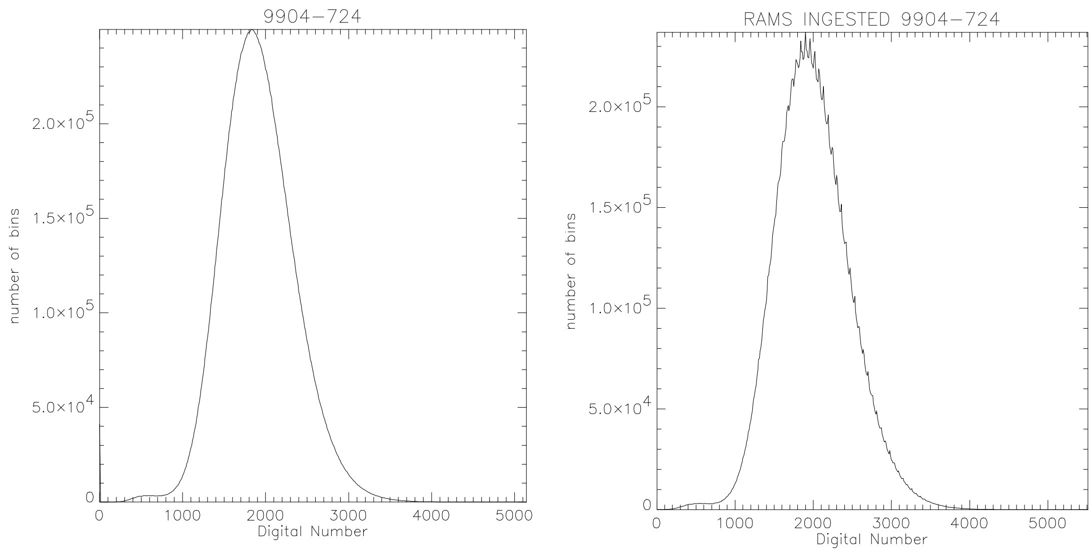


Figure 15. Histograms of original ASF DN and RAMS ingested DN (ST 2 beam)

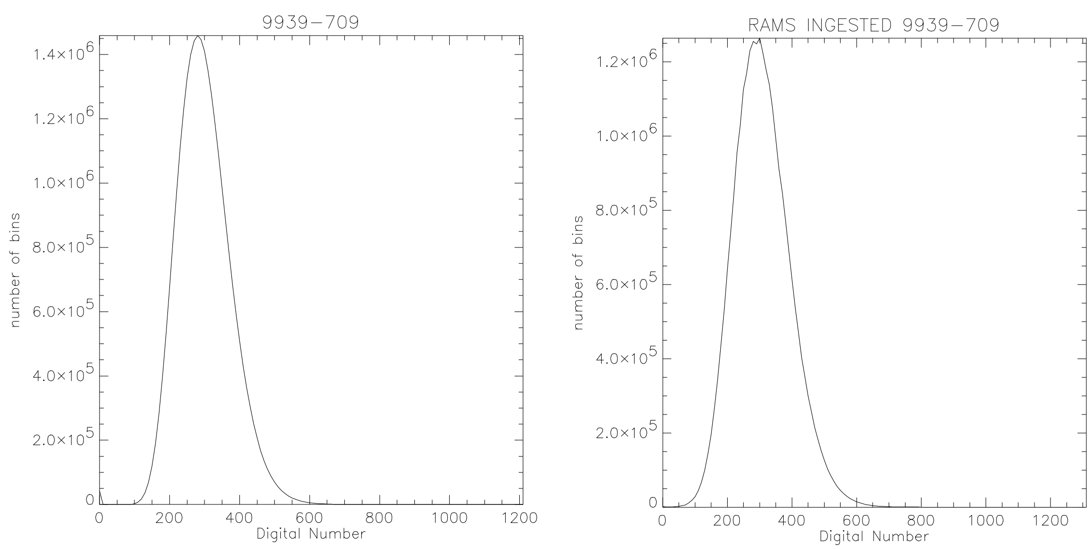


Figure 16. Histograms of original ASF DN and RAMS ingested DN (ST 2 beam)

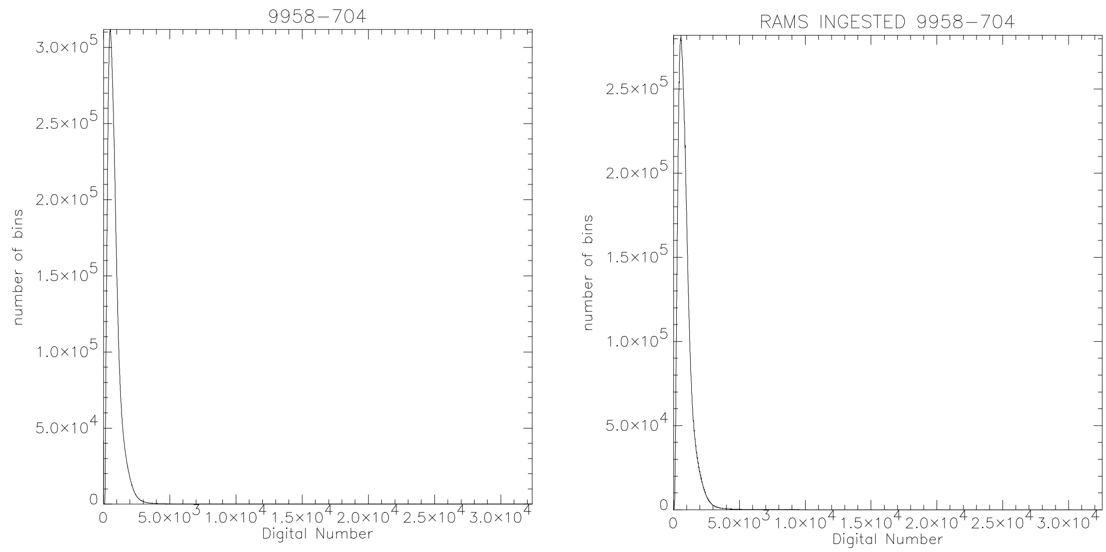


Figure 17. Histograms of original ASF DN and RAMS ingested DN (ST 2 beam)

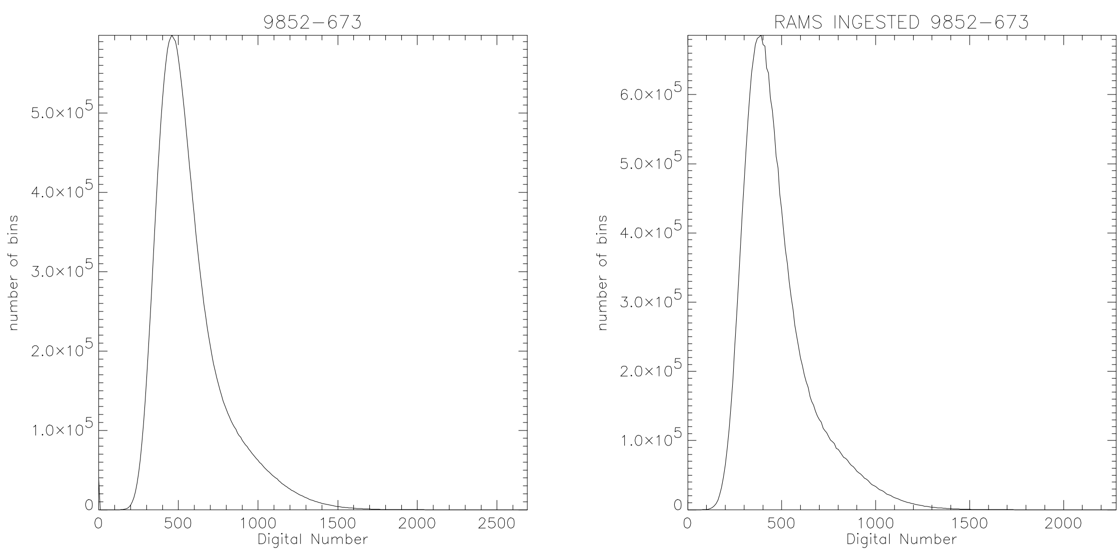


Figure 18. Histograms of original ASF DN and RAMS ingested DN (ST 3 beam)

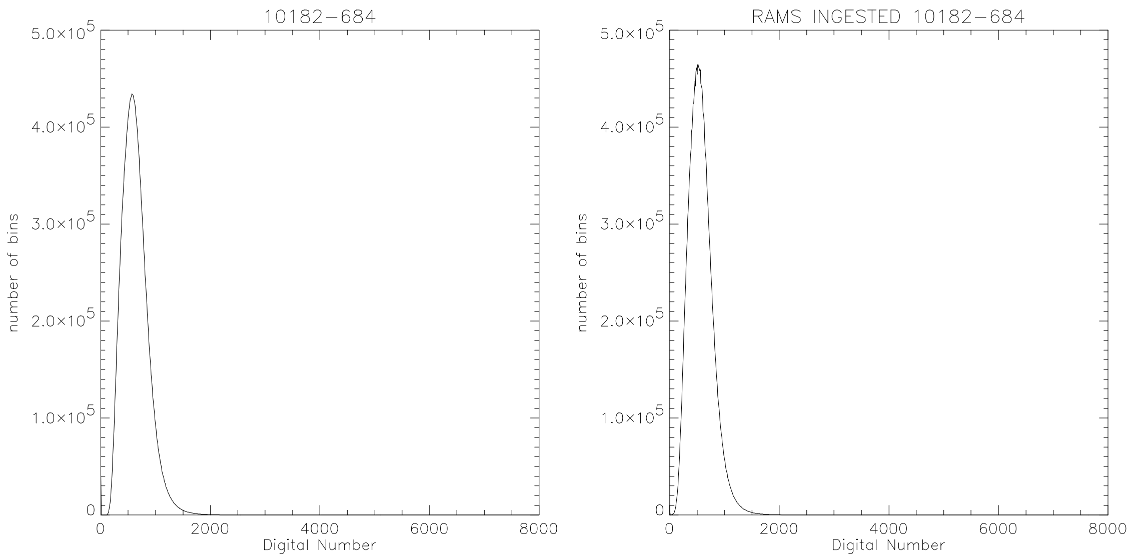


Figure 19. Histograms of original ASF DN and RAMS ingested DN (ST 4 beam)

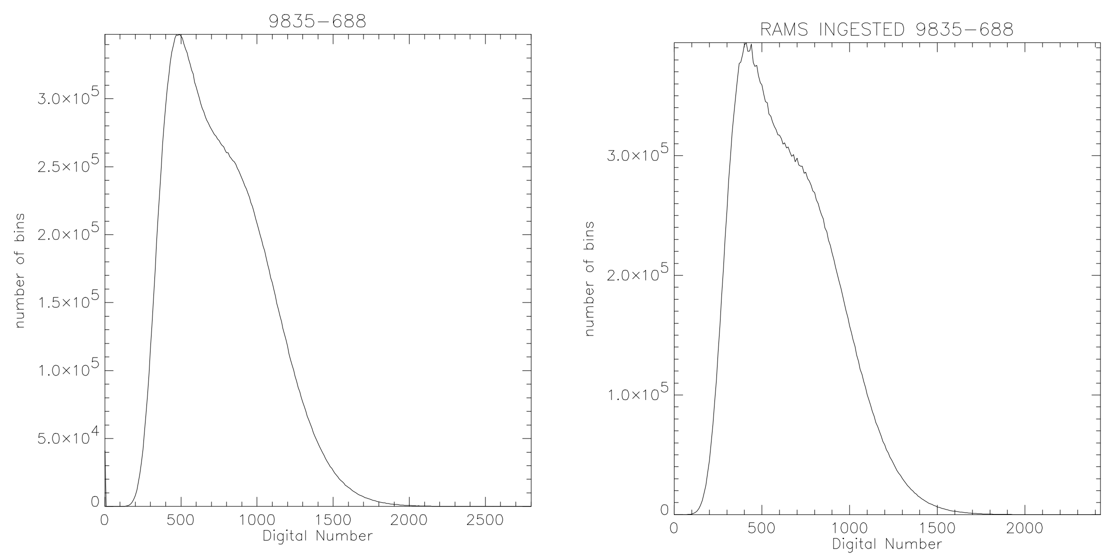


Figure 20. Histograms of original ASF DN and RAMS ingested DN (ST 5 beam)

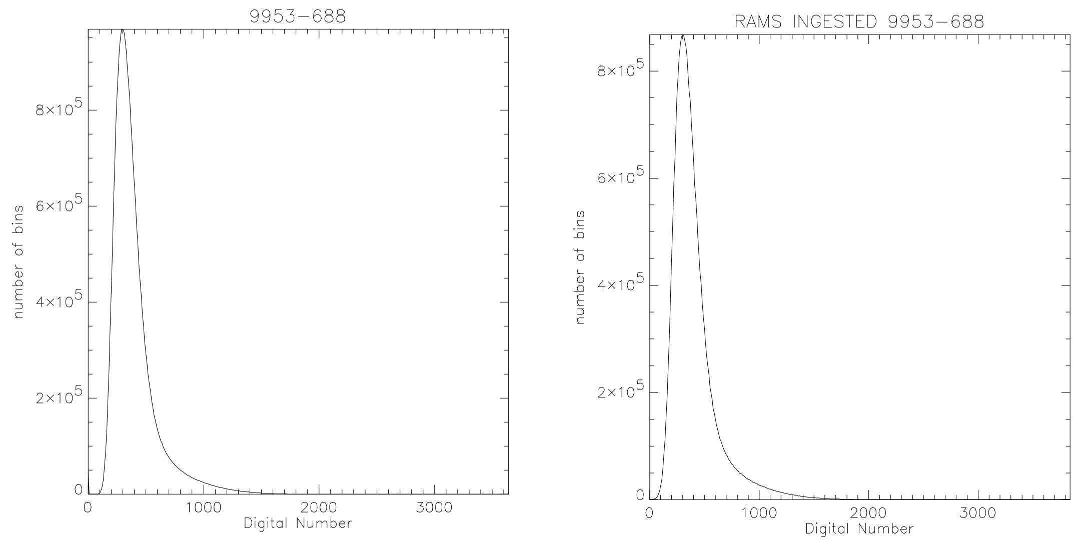


Figure 21. Histograms of original ASF DN and RAMS ingested DN (ST 6 beam)

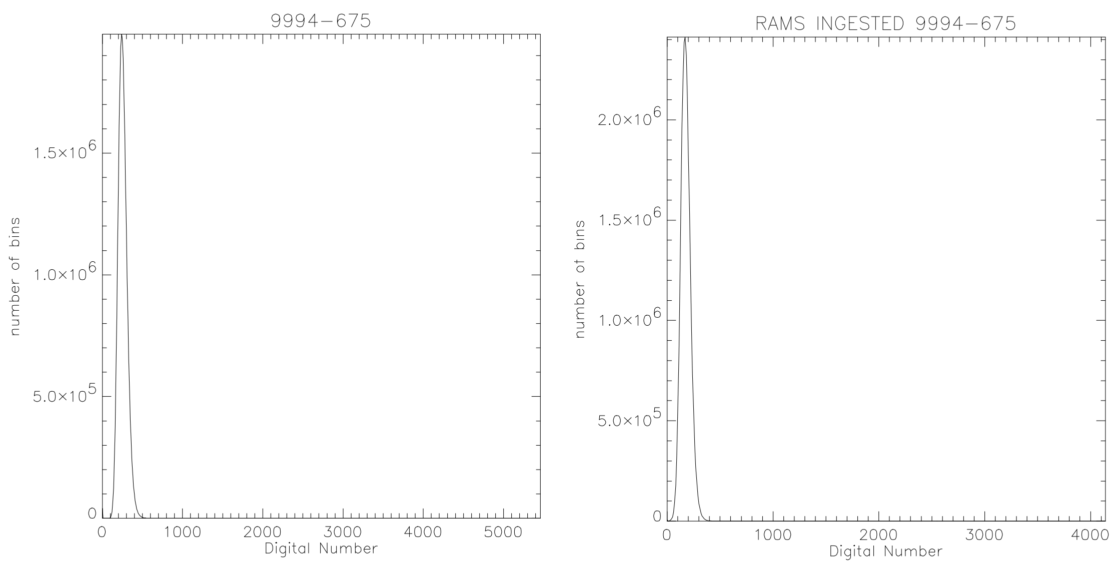


Figure 22. Histograms of original ASF DN and RAMS ingested DN (EH 4 beam)

## REFERENCES

Kipple, A., 1998, AMM Calibration Report, Alaska SAR Facility, 14-July-98.

Rott, H. and W. Rack, 1995, Characterization of Antarctic Firn by Means of ERS-1 Scatterometer Measurements, IGARSS'95, pp. 2041-2043.

Rott, H. K. Sturm, and H. Miller, 1993, Active and passive microwave signatures of Antarctic firn by means of field measurements and satellite data, Annals of Glaciology, Vol. 17, pp. 337-343.

Ulaby, F.T., R.K. Moore, and A.K. Fung, 1983, Microwave Remote Sensing, Vol II, Addison-Wesley Publishing Co.